Rational Design of Immunostimulatory siRNAs

Michael P Gantier[1,6], Stephen Tong[1,2,6], Mark A Belhke[3], Aaron T Irving[1], Martha Lappas[4], Ulrika W Nilsson[1], Nigel AJ McMillan[5] and Bryan RG Williams[1]

[1]Centre for Cancer Research, Monash Institute of Medical Research, Monash University, Melbourne, Victoria, Australia; [2]Centre for Women's Health Research, Monash Institute of Medical Research, Monash University, Melbourne, Victoria, Australia; [3]Integrated DNA Technologies, Coralville, USA, [4]University Department of Obstetrics and Gynaecology, Mercy Hospital for Women, Melbourne, Victoria, Australia; [5]University of Queensland Diamantina Institute for Cancer, Immunology and Metabolic Medicine, Brisbane, Queensland, Australia; [6]Both authors contributed equally to this article.

Correspondence: Bryan Williams, Centre for Cancer Research, Monash Institute of Medical Research, Monash Medical Centre, 246 Clayton Road, Clayton, Victoria 3168, Australia. Email: Bryan.Williams@med.monash.edu.au

Tel: +61 3 9594 7100 Fax: +61 3 9594 7114

Short title: Design of immunostimulatory siRNAs

ABSTRACT

Short interfering RNAs (siRNAs) have engendered much enthusiasm for their ability to silence expression of specific genes. However, it is now well established that siRNAs, depending on their sequence, can be variably sensed by the innate immune system through recruitment of toll-like receptors 7 and 8 (TLR7/8). Here we aimed to identify sequence-based modifications allowing for the design of bifunctional siRNAs with both pro-inflammatory and specific silencing activities, and with potentially increased therapeutic benefits as antiviral or antitumor agents. We found that the introduction of a micro-RNA-like non-pairing uridine-bulge in the passenger strand robustly increased immunostimulatory activity on human immune cells. This sequence modification had no effect on the silencing efficiency of the siRNA. Increased immunostimulation with the uridine-bulge design was specific to human cells, and conserved silencing efficiency required a Dicer-substrate scaffold. The increased cytokine production with the uridine-bulge design resulted in enhanced protection against Semliki Forest virus infection, in viral assays. Thus, we characterize for the first time a design scaffold applicable to any given siRNA sequence, that results in increased innate immune activation without affecting gene silencing. This sequence coupled with structural modification differentially recruits human TLR8 over TLR7, and could have potential application in antiviral therapies.

INTRODUCTION

RNA interference (RNAi) is an evolutionarily conserved antiviral mechanism that relies on short molecules of double-stranded RNA (dsRNA) of 21-23 base pairs (bp), known as short interfering RNAs (siRNAs). Among species, the hallmark of RNAi is its specificity, affecting only the expression of the target gene sharing perfect homology with the siRNA sequence. Several siRNAs targeting disease-causing genes are currently in clinical trials, and the therapeutic potential of these double-stranded oligoribonucleotides is extensive.[1] However, we and others have shown that siRNAs can be sensed by the mammalian immune system, compromising the specificity of silencing.[2-4] In addition to the recognition of low-molecular-mass synthetic agonists such as imidazoquinolines, toll-like receptors 7 and 8 (TLR7/8) can sense single-stranded RNAs (ssRNAs) and siRNAs in a sequence-specific manner.[2, 3, 5] Recent publications indicate that short RNAs can be differentially sensed by TLR7 and TLR8, according to their sequence.[6, 7] The expression of these receptors is restricted to certain blood immune cell subtypes, including human plasmacytoid dendritic cells (pDCs) which express the highest levels of TLR7, and human monocytes/macrophages which express the highest levels of TLR8.[8] Systemic delivery of siRNA *in vivo* is intrinsically related to a potential recruitment of these immune cells, as both TLR7 and 8 are located in the endosomal compartment and can sense endocytosed ssRNA/dsRNA.[9] TLR7 activation in pDCs preferentially induces interferon-α (IFN-α) production, whereas TLR8 activation in monocytes/macrophages results in production of tumor necrosis factor-α (TNF-α) and interleukin-12(p70) (IL-12(p70)).[10]

While immune activation caused by siRNAs was unanticipated and is a cause of concern,[11] backbone modifications have been developed that dampen activation of an immune response.[12-14] However, we have previously proposed that it might be therapeutically beneficial to

design siRNAs that provoke an enhanced immune response and enhance siRNA-mediated antiviral and antitumor therapy.[11] Indeed, proof of principle of a "bifunctional" siRNA approach of combining gene silencing and immunostimulation demonstrating antitumoral synergy between innate immune recruitment and gene-specific targeting has recently published.[15] However, this study relied on a 5'-triphosphate modification of siRNA and activation of innate immunity via retinoic acid-inducible gene I (RIG-I).[15]

To date, there are several reports that certain motifs in siRNA duplexes specifically induce TLR7/8,[2, 3] and detailed studies of 19-21 nucleotide (nt) single-stranded RNAs have identified different motifs that promote TLR7/8 recruitment ([6], European patents EP1764107 and EP1764108). While useful, determination of immunostimulatory motifs in each individual strand of an siRNA is a poor predictor of the immunostimulatory potential of the resulting duplex ([4, 16] and Gantier and Williams, unpublished). Importantly, rational design of efficient siRNAs remains predictive, and in most cases only a few siRNAs can be confirmed to promote strong silencing. Selection of siRNAs based on criteria of both RNAi efficiency and sequenced-based immunostimulatory potential may compromise one or other parameter. To our knowledge, there is currently no modification described that can be applied to a given siRNA duplex to increase its ability to recruit TLR7/8 without impacting on its gene silencing efficiency. Here we characterize a micro-RNA (miRNA)-like sequence modification that robustly increases immunostimulation of three independent Dicer-substrate siRNAs (D-siRNAs). This modification did not impact on silencing efficiency of the duplexes, and likely involves specific TLR8 recruitment.

RESULTS

Structural/sequence requirements of short RNAs for TLR7/8 activation

We and others have previously demonstrated that TLR7/8 sensing of short RNAs is uridine dependent.[5, 7, 17] However, our previous findings also indicated that the position of the uridine residues within the secondary structure of an ssRNA could impact on immunostimulation.[7] To further characterize the impact of secondary structure of ssRNAs on TLR7/8 recruitment, we used a rational approach to increase the predicted self-complementarity of an ssRNA previously shown to activate both IFN-α and TNF-α in human peripheral blood mononuclear cells (PBMCs), without affecting its uridine content (B-406-AS [7]) (Fig. 1a and Table 1). Increasing the secondary structure did not significantly affect IFN-α, but it strongly impacted on the TNF-α induction profile in human PBMCs (>2-fold increase for B-406AS-1 and B-406AS-2 compared to B-406AS, Figs. 1a and b). Surprisingly, restriction of the 5 nt loop of B-406AS-2 to a 3 nt loop (see B-406AS-3) ablated the TNF-α induction seen in B-406AS-2. Taken together, these results suggested that TLR8 (as measured through TNF-α production) was more sensitive to the secondary structure of an ssRNA than TLR7 (measured through IFN-α production). In parallel, we also assessed the net impact of uridine content in an ssRNA with low self-secondary structure, independent of structure variation (Fig. 1c and Table 1). In accord with uridine-dependent TLR7/8 sensing, both IFN-α and TNF-α were induced in a dose-dependent manner with increasing uridines (Fig. 1d, compare ss41-N and ss41-4/6/8/10). At the doses of ssRNA used (90 nM), a minimum of four uridines was required to detect immunostimulation (see ss41-4, for TNF-α), consistent with our previous observations (see SC and SB ssRNAs [7]). However, more than eight uridines did not result in any further increase in cytokine production (compare ss41-8

and ss41-10, for IFN-α and TNF-α, Fig. 1d). Collectively, these results support a role for both uridine content and secondary structure in TLR7/8 sensing of ssRNAs.

Rational design of immunostimulatory siRNAs

To study the impact of uridine content and secondary structure of siRNA duplexes on both immunostimulation and silencing efficiency, we used a rational approach affecting the sequence of siRNA duplexes. While siRNAs are conventionally designed as 21-23 bp duplexes to mimic Dicer products, it has been shown that dsRNAs that are long enough to be treated as Dicer substrates (D-siRNAs) can also promote RNAi in mammalian cells.[18, 19] Further, using an asymmetric D-siRNA of 25/27 nt with both blunt and 3' overhang ends helps to mimic the natural substrates of mammalian Dicer (i.e. pre-miRNA hairpins) and allows for increased directional processing and selection of the guide strand of the siRNA.[18, 19] The 3' end of an asymmetric D-siRNA (using the passenger strand as a reference) is preferentially cleaved by Dicer and should have little impact on sequence-specific silencing.[18] Accordingly, a set of three D-siRNAs was synthesized with increased uridines in the region predicted to be cleaved by Dicer (siLam-1, siLam-2, siLam-3, Fig. 2a). Noting that TLR8 may be sensitive to the secondary structure of ssRNAs (Fig. 1), we designed a Dicer substrate with a miR-29a-like uridine-bulge on the passenger strand (position 9-12), predicting that this modification would not alter Dicer processing and strand selection (siLam-4, Fig. 2a). These siRNAs were derived from a previously validated D-siRNA sequence targeting the human *LaminA/C* (LMNA) mRNA (M. Behlke, unpublished). Unexpectedly, when assayed for immunostimulation in human PBMCs, a decrease in IFN-α and/or TNF-α levels with siLam-1 and siLam-2 was observed when compared to the

native siLam control (Fig. 2b). Nevertheless, both siLam-3 and siLam-4 promoted a significant increase in IFN-α and/or TNF-α production. In HEK 293T cells, siLam-2 and siLam-4 both silenced *LaminA/C* mRNA expression with equal efficacy to the control sequence, but the other approaches were less effective (Fig. 2c). siLam-4 silencing efficacy was confirmed by measuring *LaminA/C* mRNA silencing by siLam-4 compared to control siLam-N in dose-response experiments (at 10 nM, 2 nM and 0.4 nM), where no significant differences were observed (not shown). These results indicated that the addition of an miRNA-like uridine-bulge to a D-siRNA scaffold resulted in increased immunostimulation without affecting RNAi activity.

Validation of the uridine-bulge siRNA design

In order to validate that the previous observations made with the siLam-4 design could be reproduced independently of the sequence of the duplex/target chosen, a D-siRNA targeting the enhanced green fluorescent protein (EGFP) was selected using the siRNA design software BIOPREDsi.[20] From the five best hits suggested by BIOPREDsi, the duplex with the least number of uridine residues was selected to minimize the basal immunostimulatory activity of the siRNA, and 6 nt complementary to the EGFP target added to make it a D-siRNA (Fig. 3e). When comparing this EGFP D-siRNA with (siEGFP-U) or without (siEGFP) the bulge modification in immunostimulatory assays, a strong increase in TNF-α induction (>10 fold at 500 and 750 nM) and a significantly higher induction of IFN-α (at 500 nM) with the uridine-bulge modification was observed (Fig. 3a). In addition, the uridine-bulge did not affect the ability of the EGFP D-siRNA to trigger RNAi in HEK 293T cells stably expressing EGFP (Fig. 3b). Similar results were seen with another D-siRNA target, the *E6/E7* oncogene of the Human Papilloma Virus 16

(Figs. 3c, d and e, compare siE6/E7 and siE6/E7-U). Collectively, these results support the findings that independent of the D-siRNA sequence, the uridine-bulge design robustly increases TNF-α and IFN-α induction in human PBMCs, without altering the ability of the D-siRNA to enter the RNAi pathway.

Uridine-bulge sensing is not conserved between human and mouse

The preferential induction of TNF-α over IFN-α with the uridine-bulge modification of all D-siRNAs suggested a predominant role for monocytes in sensing the bulge. To better define the immune cell subtype involved in the sensing of the modification, the ability of isolated CD14+ monocytes to respond to the uridine-bulge of siEGFP-U was assessed (Fig. 4a). As anticipated, a significantly increased production of TNF-α was observed with the uridine-bulge D-siRNA (siEGFP-U) (>15 fold) in these cells. We have recently reported that human monocytic cells sense short RNAs through both TLR7 and TLR8 recruitment.[7] To further characterize the respective involvement of both receptors in the sensing of the uridine-bulge modification, we used mouse bone marrow derived macrophages (BMMs), in which ssRNA/siRNA sensing exclusively relies on TLR7 due to the lack of mouse TLR8 response to RNA agonists.[2, 5, 7] Unexpectedly, the uridine-bulge modification inhibited rather than promoted the immunostimulatory effect of the siEGFP D-siRNA, as measured by TNF-α production (Fig. 4b). While this implicates human TLR8 in sensing of the uridine-bulge modification, it precludes using murine-based disease models to measure potential therapeutic benefits of the uridine-bulge modification.

Pro-inflammatory/antiviral effects of uridine-bulge modification

We next looked to elucidate the cytokine profile induced by the uridine-bulge modification of the three D-siRNAs (siLam-4, siEGFP-U and siE6/E7-U) in human PBMCs. Multi-cytokine protein array analysis of 17 cytokines confirmed significant up-regulation of the pro-inflammatory cytokines TNF-α, IFN-γ, IL-1β, and IL-12(p70) (Fig. 5). In addition, IL-4, IL-5, IL-7, IL-10, IL-17, G-CSF and GM-CSF were also significantly induced in at least two of the three D-siRNAs analyzed (not shown). Notably, both the IL-6 and IL-8 values were outside the linear range of the standard curve and were not accurately assessed. Since there was increased induction of type I and II IFNs by the uridine-bulge modification, the antiviral effects of the modified siEGFP D-siRNAs were assessed. Conditioned media from PBMCs treated overnight with the EGFP D-siRNAs was used to treat Hela cells prior to infection with Semliki Forest virus (SFV) and Hela cell survival was subsequently assayed (*Materials and Methods*). As expected from the higher IFN-α production (Fig. 3), the results showed that the uridine modification of siEGFP-U conferred significant protection to viral infection compared to the native siEGFP D-siRNA (Fig. 6).

Use of uridine-bulge modification with 21 bp siRNA scaffold

siβ-Gal-924 is a 21 bp siRNA duplex targeting the *β-galactosidase* mRNA, demonstrating silencing efficiency but low immunostimulatory potential in human PBMCs.[3] To define whether the uridine-bulge modification could also be applied independently of the Dicer-substrate scaffold, we synthesized siβ-Gal-924 and its uridine-bulge variant (siβ-Gal-924-U, Supplementary Table S1) and tested for immunostimulation and down-regulation efficiency. In

agreement with our previous results, the uridine-bulge modification of siβ-Gal-924 promoted significant induction of TNF-α and IFN-α in human PBMCs, compared to its native variant (Fig. 7a). Nevertheless, in HEK 293T cells transiently expressing β-galactosidase, the down-regulation efficiency of siβ-Gal-924 was reduced (~10%) by the uridine-bulge modification, indicating an adverse effect of the modification on RNAi recruitment (Fig. 7b). Of note, siβ-Gal-478 promoted stronger down-regulation of β-galactosidase than siβ-Gal-924, as previously reported.[3]

DISCUSSION

The innate immune system is the first line of defense against infection with viruses or pathogens. Sensing of specific pathogen-associated molecular patterns (PAMPs) by innate immune receptors such as the TLRs, is followed by the induction of a targeted response limiting the infection. As key mediators of this response, IFNs coordinate the expression of hundreds of antiviral genes.[21] For this reason, IFNs are commonly used in the treatment of hepatitis C (HCV) or chronic hepatitis B virus (HBV) infection.[22, 23] Recruitment of TLR7 or both TLR7 and 8 by synthetic agonists (such as isatoribine and resiquimod) potently induces IFNs, and reduces HCV plasma virus concentration.[24]

The use of siRNAs or RNAi-based therapies in the treatment of chronic viral infections such as immunodeficiency virus type 1 (HIV-1), HCV and HBV is currently under intense scrutiny and promises to overcome the limitations of currently available treatments.[25-27] Given that IFNs are antiviral, it is reasonable to assume that in certain viral infections a strategy aimed at recruiting TLR7/8 together with specific gene silencing could have a therapeutic effect on viral clearance.[27] In support of this, two groups have recently demonstrated the antiviral effects promoted by sequence-specific siRNA recruitment of TLR7 in murine models of Influenza infection.[28, 29] In addition, dual recruitment of antiviral RNAi and TLR7/8 by siRNAs can be achieved *in vivo*, as shown by Morrissey et al.[30] This group demonstrated RNAi-driven specific reduction of HBV replication, together with a TLR7-driven antiviral response with the same siRNA-lipid delivery system.[30]

In this work, we sought to develop siRNAs with enhanced immunostimulatory potential via TLR7/8 activation. The finding that TNF-α but not IFN-α was strongly induced when self-

complementarity was added to a single-stranded short RNA in human PBMCs (Fig. 1b), led us to speculate that TLR7 and TLR8 sensing of short RNAs is governed by a different sensing of secondary structures. Further, the observation that the introduction of an miRNA-like uridine-bulge in the middle of an siRNA duplex consistently induced increased immunostimulation in human monocytes (Fig. 4a) but not in mouse macrophages (Fig. 4b), suggests that human TLR8 and not TLR7, is the sensor of the uridine-bulge modification. In agreement with this, a recent study by Ablasser *et al.* showed a TLR8-activation-dependent increase in production of IL-12(p70), following introduction of mismatches in the strands of an siRNA duplex.[10] Unexpectedly, the introduction of additional uridines in the 3' end of a D-siRNA (using the passenger strand as reference) decreased immunostimulation when the Watson-Crick base pairing was conserved (Fig. 2, siLam-1 and siLam-2). Nonetheless, the loose secondary structure of this 5' end region with G:U wobble pairing resulted in increased TNF-α, independent of IFN-α (Fig. 2, siLam-3). Whilst confirming a role for uridines in TLR7/8 sensing (Fig. 1), our results emphasize that the immunostimulatory potential of an siRNA duplex cannot be accurately predicted through sequence analysis. In support of our findings, a screen of 207 siRNAs for TLR7/8 stimulation in human PBMCs recently suggested that in addition to uridine content, decreased strength of hybridization between the two complementary strands of an siRNA duplex positively correlated with increased immunostimulatory activity.[31] The results from our three distinct siRNA duplexes are unequivocal: addition of the uridine-bulge promotes increased TNF-α, IFN-γ, IL-1β, and the Th1 polarizing IL-12(p70) (Fig. 5). However, we also observed possible saturation in the immunostimulation conferred by the uridine-bulge with one siRNA sequence exhibiting high basal immunostimulatory potential (Supplementary Fig. S1 – compare siEGFP-U 500 nM and siBcl2l12-N 250 nM). Based on these results, we propose that the addition of the

uridine-bulge modification will increase pro-inflammatory activation of any given siRNA sequence that is not already strongly immunostimulatory, most likely through human TLR8.

The measurement of both mRNA and protein levels of targeted genes indicated that while the uridine-bulge did not impact on the silencing efficiency of any of the Dicer-substrate siRNAs studied (Figs. 2c, 3b and 3d), it significantly inhibited RNAi when used in the context of a 21 bp siRNA scaffold (Fig. 7b). Relying on the consistent observation that the bulge did not alter silencing on three different D-siRNAs, it is unlikely that the difference observed with the shorter β-galactosidase uridine-siRNA is simply related to this particular sequence. Because the two scaffold designs compared here differ only from one another by their position in the Dicer processing step (i.e. upstream or downstream of Dicer), it can be speculated that Dicer processing and direct recruitment of the bulge-siRNA is required for correct unwinding and RNA induced silencing complex (RISC) loading of the imperfect miRNA-like siRNA duplex. However, it could also be argued that the lower affinity of the two strands destabilizes the 21 bp bulge β-galactosidase siRNA duplex and renders it more prone to degradation, while the longer conformation of the D-siRNAs would confer protection. Our observation that the bulge modification of the D-siRNAs did not affect RNAi efficiency when compared to a perfectly pairing duplex was unexpected. It is currently thought that perfectly pairing duplexes undergo Ago2 processing of the passenger strand,[32] while miRNA-like imperfect duplexes would be unwound through an elusive helicase.[33] The finding that similar RNAi efficiency can be achieved regardless of the affinity of the two strands of a D-siRNA highlights the concept that Ago2-RISC cleavage efficiency of the complementary target is not affected by the nature of the prior degradation or unwinding of the passenger strand of the duplex, when Dicer is involved in active RISC formation. Further in-depth investigations of the role of Dicer in the recruitment of RNAi

by bulge-modified siRNAs with the two scaffold designs should help better characterize the previous findings, and could be informative in the design of better miRNA mimics.

SFV is a single-stranded positive-sense Alphavirus that induces apoptosis of continuously cultured cells 24-48 hours after infection.[34] SFV is particularly sensitive to IFN pre-treatment of cells prior to infection.[35] Here we found that conditioned media from human PBMCs treated with a uridine-bulge D-siRNA conferred increased protection to SFV infection of Hela cells, when compared to a perfect D-siRNA duplex (Fig. 6). This can be attributed to IFN-α production by the PBMCs and demonstrates that the increased immunostimulatory potential conferred by the uridine-bulge modification can have potent antiviral benefits. However, because the increased immunostimulatory effects of the uridine-bulge were not reproduced in mouse due to mouse TLR8 unresponsiveness to ss/siRNAs [5]), we were unable to further characterize the benefits of the uridine-bulge modification *in vivo*.

In conclusion, we provide here the first rational design of a bifunctional D-siRNA scaffold, which can be applied to any given siRNA sequence. We demonstrate that the addition of an miRNA-like uridine-bulge to a Dicer substrate siRNA duplex confers increased immunostimulation in human PBMCs, with potential protective effect in viral infection. The bulge modification does not compromise RNAi recruitment and target-specific down-regulation, when used in a D-siRNA scaffold. Our data is indicative of a TLR8-preferential recruitment of short RNAs with loose secondary structure, including D-siRNAs with the uridine-bulge modification. Because it relies on a sequence modification, the uridine-bulge strategy presented in this work could be immediately amenable to large-scale industrial production of oligoribonuclotides, unlike other proposed modifications such as the 5'-triphosphate.[15] Combined target-specific delivery of bifunctional uridine-bulge D-siRNAs together with macrophage uptake

could therefore have therapeutic benefits in the treatment of viral infections and potentially other diseases, including cancer.

MATERIALS AND METHODS

Cell isolation and culture. Fresh blood from healthy male donors was collected in heparin-treated tubes and PBMCs separated by ficoll-paque plus (#17-1440-02, GE Healthcare, Rydalmere, Australia) gradient purification, and plated in a 96-well plate at $2x10^5$ cells per well in RPMI 1640+L-glutamine medium (#11875085, Invitrogen Corporation, Carlsbad, CA) complemented with 1x antibiotic/antimycotic (#15240062, Invitrogen Corporation) and 10% fetal bovine serum (#FBS-500, ICPBio Ltd, Auckland, New Zealand) (referred to as complete RPMI), as previously reported.[7] For the purification of CD14+ monocytes, flow cytometric sorting of PBMCs was carried out using anti-CD14-PE (#555398, BD Biosciences, San Jose, CA) as previously reported.[36] HEK 293T cells and their GFP stable variant (gift from A. Sadler, Monash Institute of Medical Research, Melbourne, Australia), were cultured in complete DMEM (#11965-092; Invitrogen Corporation) supplemented with 10% sterile FBS and 1x antibiotic/antimycotic. TC-1 cells, a murine fibroblast cell line expressing the human papilloma virus 16 (HPV), were grown in complete DMEM.

Isolation of bone marrow macrophages. Mice were housed at the Monash animal facility (Monash University, Clayton campus, Australia) and approved under MMCA2007/07. Femurs were collected and flushed with RPMI, and cells were plated in complete RPMI supplemented with 20% L929-cell conditioned medium on 10 cm bacteriological plastic plates for 7 days at 37°C in a 5% CO_2 atmosphere.

Cell stimulation. All siRNA duplexes were synthesized as single-stranded RNAs by Integrated DNA Technologies (IDT) with HPLC purification, and resuspended in duplex buffer (100 mM potassium acetate, 30 mM HEPES, pH 7.5, DNase–RNase free H_2O) to a concentration of 80 μM. ssRNAs were annealed to form siRNA duplexes at 92°C for 2 minutes and left for 30 minutes at room temperature before aliquoting (giving a final concentration of 40 μM). 3M-002 (human TLR8 agonist and mouse TLR7 agonist [7]) (#tlrl-c75) and ODN2216 (TLR9 agonist) (#tlrl-hodna) were purchased from Invivogen (San Diego, CA) and used at a final concentration of 1 μg/ml and 3 μM, respectively. For immunostimulation assays in PBMCs, CD14+ cells and BMMs, ss/siRNAs were transfected with DOTAP (#1811177, Roche, Nutley, NJ), as previously reported.[7] Transfections were carried out in biological triplicate in all experiments. The ratios of DOTAP to ss/siRNA were as follows: 5.3 μg/μl of 80 μM ssRNA (Figs. 1a and b) and 1.87 μg/μl of 40 μM siRNA (Figs. 2, 3, 4, 5 and 7). When dose-response experiments were carried out, the ratio of siRNA to DOTAP was kept constant.

RNA interference by reverse transfection. For Figs. 3b and 7b, 1.35 μl Lipofectamine 2000 (#11668; Invitrogen Corporation) was diluted in 150 μl of Opti-MEM (#51985-034; Invitrogen Corporation), and 1.5 μl of siRNA molecules (diluted to 4 μM in duplex buffer or freshly in Opti-MEM) was added such that the final concentration of siRNA in each well was 10 nM. After 20 minutes of incubation, 50 μl of the Lipofectamine 2000/siRNA/OptiMEM mixture was added directly into each well of a 96-well plate (in triplicate). Approximately 15,000 HEK 293T-GFP cells suspended in 150 μl of antibiotic-free DMEM (supplemented with 10% FBS) was added to each well, giving a final volume of 200 μl per well. For Figs. 2c and 3d, 4.5 μl of Lipofectamine

2000 was diluted in 300 μl of Opti-MEM and 4.5 μl of siRNA molecules (diluted to 4 μM in duplex buffer or freshly in Opti-MEM) was added such that the final concentration of siRNA in each well was 10 nM. After 20 minutes of incubation, 50 μl of the mix was added directly into each well of a 24-well plate (in triplicate). 100,000 HEK 293T cells or TC-1 cells resuspended in 500 μl of antibiotic-free DMEM (supplemented with 10% FBS) was added to each well giving a final volume of 600 μl per well. For the Mock condition, no siRNA was added to the Lipofectamine mix, while for the Medium condition, OptiMEM only was added to the wells (i.e. no Lipofectamine or siRNA was added). siControl is a non-targeting siRNA control (#4635, Ambion, Austin, TX), and siGFP19+2 is a published 21 bp siRNA molecule previously shown to down-regulate EGFP expression.[4]

Real-time RT-PCR. cDNA was synthesized from column-purified RNA (NucleoSpin RNAII columns, #740955, Macherey-Nagel Inc., Bethlehem, PA) using the SuperScript III First-Strand Kit (#18080-051, Invitrogen Corporation), with random hexamer priming and following the manufacturer's instructions. Real-time PCR was carried out with the SYBR GreenER™ qPCR SuperMix for iCycler® instrument (#11761-500; Invitrogen Corporation). *hGAPDH* (NM_002046) and *mGAPDH* (NM_008084) were used as reference and were amplified with the following primer pairs, respectively: hGAPDH-FWD: CATCTTCCAGGAGCGAGATCCC; hGAPDH-REV: TTCACACCCATGACGAACAT; mGAPDH-FWD: TTCACCACCATGGAGAAGGC; mGAPDH-REV: GGCATGGACTGTGGTCATGA. *hLaminA/C* (NM_170707) and *E6/E7* of HPV16 (FJ610149) were amplified with the following primer pairs, respectively: Lamin-FWD: AGCAAAGTGCGTGAGGAGTT; Lamin-REV: GAGTTCAGCAGAGCCTCCAG; E6-FWD: TTGCTTTTCGGGATTTATGC; E6-REV:

CAGGACACAGTGGCTTTTGA. Each amplicon was sequence verified and used to generate a standard curve for the quantification of gene expression.

Detection of cytokines. Human IFN-α in culture supernatants was quantified by sandwich ELISA using mouse monoclonal (0.5 μg/ml, #21112-1, PBL Biomedical, Piscataway, NJ) and rabbit polyclonal antibodies (0.5 μg/ml, #31130-1, PBL Biomedical). A goat anti-rabbit HRP-conjugated antibody (0.8 μg/ml, #31460, Pierce, Rockford, IL) was used for detection. Human and mouse TNF-α were measured using the BD OptEIA ELISA sets (#555212 and #558874, respectively, BD Biosciences). In both IFN-α and TNF-α ELISAs, TMB substrate (#T0440, Sigma Aldrich, St. Louis, MO) was used for quantification of the cytokines on a Fluostar OPTIMA (BMG LABTECH, Offenburg, Germany) plate-reader. For the Bio-Plex human cytokine 17-plex panel (#171-A11171, Bio-Rad laboratories, Hercules, CA), the assays were performed following the manufacturer's guidelines. A standard curve was generated for each cytokine using a five-parameter logistic regression curve fit and analyzed concentrations were determined automatically using Bio-Plex Manager software (v4.01). All results below the detectable limit were recorded as zero, and those above the standard curve were assigned a value equal to the top standard.

Fluorescent-based measure of EGFP knockdown. EGFP expression (and down-regulation) in HEK 293T-GFP cells was measured using a Fluostar OPTIMA plate-reader. RNAi experiments were performed in 96-well black plates with clear bottoms (#353948, BD Biosciences Falcon). 48 hours after siRNA treatment, the supernatants were discarded and 50 μl of PBS was added to

the cells. A standard curve was generated by serially diluting a recombinant EGFP-fusion protein (gift from D. Wang, Monash Institute of Medical Research, Melbourne, Australia) to cover a range from 150 ng/ml to 4.68 ng/ml in 50 μl PBS. The equivalent EGFP concentration in each well was then inferred from the fluorescence at ex485/em520 correlated to the standard curve.

β-galactosidase enzymatic assay. 300,000 HEK 293T cells were reverse transfected with 300 ng of pLenti4/TO/V5-GW/*lacZ* (Invitrogen Corporation) complexed to 1 μl of Lipofectamine 2000 in 100 μl of Opti-MEM, in a well of a 6-well plate. 16 hours post-transfection, the cells were collected with 300 μl TrypLE™ Express Stable Trypsin (#12604-021; Invitrogen Corporation) and 1.5 ml of antibiotic-free DMEM was added. The siRNA mixes were prepared as indicated in the *RNA interference by reverse transfection* section, and 150 μl of cells were added per well, giving a final volume of 200 μl at 10 nM. The cells were further incubated for 24 hours before being lysed for 20 minutes in 40 μl of 1x Reporter Lysis Buffer (#E2000, Promega, Madison, WI) per well. 40 μl of the 2x assay buffer was added per well, and the plate was incubated for 30-45 minutes at 37°C. The enzymatic reaction was stopped with the addition of 40 μl sodium carbonate (1 M), and the plate was read at 440 nm on a Fluostar OPTIMA plate-reader.

SFV viral assay. Hela cells were seeded into 96-well plates and incubated overnight at 37°C to reach ~100% confluency. The cells were treated with 100 μl of supernatant from siRNA-treated PBMCs. A ¼ serial dilution of the conditioned media was performed for each of the siRNA treatments. Following a 4 hour pre-treatment with conditioned media, the cells were washed and

infected with 100 µl of DMEM (10% FBS) containing 200 pfu/ml of SFV. The cells were incubated with the virus for 36 hours before being rinsed with PBS and fixed with 10% formalin for 30 minutes. The cells were further stained for 30 minutes with 0.05% crystal violet in 20% ethanol, before thorough H_2O washes and reading at 590 nm on a Fluostar OPTIMA plate reader.

Statistical analyses. Statistical analyses were carried out using GraphPad Instat version 3.05. (GraphPad Software Inc., La Jolla, CA). Two-tailed unpaired T-tests or non-parametric Mann-Whitney tests were used according to the standard deviation of the compared populations. Error bars on each figure represent the standard error of the mean. Symbols used: * $P \leq 0.05$, ** $P \leq 0.01$, *** $P \leq 0.0001$ and NS is non-significant.

ACKNOWLEDGMENTS

We are grateful to Scott Rose (Integrated DNA Technologies Inc.) for his help in the production of the RNA oligonucleotides, Paul Cameron and Vanessa Evans (Monash University, Department of Medicine, Alfred Campus, Melbourne, Australia) for their help in the purification of human monocytes, Die Wang (Monash Institute of Medical Research) for the recombinant GFP and Anthony Sadler (Monash Institute of Medical Research) for the HEK 293T-GFP cells. This work is supported by funding from the Australian NHMRC 491106 and The Arthur Wilson Fellowship from The RANZCOG Research Foundation. Stephen Tong is supported by an NHMRC Career Development Award (490970). Mark A. Behlke is employed by Integrated DNA Technologies Inc., which offers oligonucleotides for sale similar to some of the compounds described in the manuscript. IDT is however not a publicly traded company, and he does not own any shares or hold equity in IDT. MP Gantier, S Tong and BRG Williams are the inventors of the Monash University international (PCT) patent application PCT/AU2009/000175, entitled Immunostimulatory siRNA Molecules.

SUPPLEMENTARY MATERIAL

Supplementary Figure S1 Immunostimulation of siRNA targeting Bcl2L12.

The native human Bcl2L12 (NM_138639) siRNA is inherently immunostimulatory. Human PBMCs were treated with indicated concentration of indicated siRNA complexed with DOTAP and incubated for 16 hours at 37°C. TNF-α concentration was measured by ELISA. The data is averaged from two independent experiments in biological triplicate from two blood donors.

Supplementary Table S1 Sequences of dsRNAs used in the study

Name	Sequence
siβ-Gal-924	5′ UUAUGCCGAUCGCGUCACAtt 3′ 3′ ttAAUACGGCUAGCGCAGUGU 5′
siβ-Gal-924-U	5′ UUAUGCCG**UUUU**CGUCACAtt 3′ 3′ ttAAUACGGCUAGCGCAGUGU 5′
siBcl2L12	5′ GCUGGUCCGCCUGUCCUCCGACUCU 3′ 3′ UUCGACCAGGCGGACAGGAGGCUGAGA 5′
siBcl2L12-U	5′ GCUGGUCC**UUUU**GUCCUCCGACUCU 3′ 3′ UUCGACCAGGCGGACAGGAGGCUGAGA 5′

The uridine-bulge is highlighted in bold and the non-matching residues are underlined.

Uppercase letters are RNA bases and lowercase letters are DNA bases.

REFERENCES

1. Castanotto D, Rossi JJ. The promises and pitfalls of RNA-interference-based therapeutics. *Nature* 2009; **457**(7228)**:** 426-433.

2. Hornung V, Biller MG, Bourquin C, Ablasser A, Schlee M, Uematsu S *et al.* Sequence-specific potent induction of IFN-alpha by short interfering RNA in plasmacytoid dendritic cells through TLR7. *Nat Med* 2005; **11**(3)**:** 263-270.

3. Judge AD, Sood V, Shaw JR, Fang D, McClintock K, MacLachlan I. Sequence-dependent stimulation of the mammalian innate immune response by synthetic siRNA. *Nat Biotechnol* 2005; **23**(4)**:** 457-462.

4. Zamanian-Daryoush M, Marques JT, Gantier MP, Behlke MA, John M, Rayman P *et al.* Determinants of cytokine induction by small interfering RNA in human peripheral blood mononuclear cells. *J Interferon Cytokine Res* 2008; **28**(4)**:** 221-233.

5. Heil F, Hemmi H, Hochrein H, Ampenberger F, Kirschning C, Akira S *et al.* Species-specific recognition of single-stranded RNA via toll-like receptor 7 and 8. *Science* 2004; **303**(5663)**:** 1526-1529.

6. Forsbach A, Nemorin JG, Montino C, Muller C, Samulowitz U, Vicari AP *et al.* Identification of RNA sequence motifs stimulating sequence-specific TLR8-dependent immune responses. *J Immunol* 2008; **180**(6)**:** 3729-3738.

7. Gantier MP, Tong S, Behlke MA, Xu D, Phipps S, Foster PS *et al.* TLR7 Is Involved in Sequence-Specific Sensing of Single-Stranded RNAs in Human Macrophages. *J Immunol* 2008; **180**(4)**:** 2117-2124.

8. Gantier MP, Williams BR. The response of mammalian cells to double-stranded RNA. *Cytokine & growth factor reviews* 2007; **18**(5-6)**:** 363-371.

9. Schlee M, Hornung V, Hartmann G. siRNA and isRNA: two edges of one sword. *Mol Ther* 2006; **14**(4)**:** 463-470.

10. Ablasser A, Poeck H, Anz D, Berger M, Schlee M, Kim S *et al.* Selection of molecular structure and delivery of RNA oligonucleotides to activate TLR7 versus TLR8 and to induce high amounts of IL-12p70 in primary human monocytes. *J Immunol* 2009; **182**(11)**:** 6824-6833.

11. Marques JT, Williams BRG. Activation of the mammalian immune system by siRNAs. *Nat Biotechnol* 2005; **23**(11)**:** 1399-1405.

12. Behlke MA. Chemical modification of siRNAs for in vivo use. *Oligonucleotides* 2008; **18**(4)**:** 305-319.

13. Robbins M, Judge A, Liang L, McClintock K, Yaworski E, MacLachlan I. 2'-O-methyl-modified RNAs act as TLR7 antagonists. *Mol Ther* 2007; **15**(9)**:** 1663-1669.

14. Judge AD, Bola G, Lee ACH, MacLachlan I. Design of Noninflammatory Synthetic siRNA Mediating Potent Gene Silencing in Vivo. *Molecular Therapy* 2006; **13:** 494-505.

15. Poeck H, Besch R, Maihoefer C, Renn M, Tormo D, Morskaya SS *et al.* 5'-Triphosphate-siRNA: turning gene silencing and Rig-I activation against melanoma. *Nat Med* 2008; **14**(11)**:** 1256-1263.

16. Sioud M. Single-stranded small interfering RNA are more immunostimulatory than their double-stranded counterparts: a central role for 2'-hydroxyl uridines in immune responses. *European journal of immunology* 2006; **36**(5)**:** 1222-1230.

17. Diebold SS, Massacrier C, Akira S, Paturel C, Morel Y, Sousa CR. Nucleic acid agonists for Toll-like receptor 7 are defined by the presence of uridine ribonucleotides. *European journal of immunology* 2006; **36:** 3256-3267.

18. Amarzguioui M, Lundberg P, Cantin E, Hagstrom J, Behlke MA, Rossi JJ. Rational design and in vitro and in vivo delivery of Dicer substrate siRNA. *Nature protocols* 2006; **1**(2)**:** 508-517.

19. Rose SD, Kim DH, Amarzguioui M, Heidel JD, Collingwood MA, Davis ME *et al.* Functional polarity is introduced by Dicer processing of short substrate RNAs. *Nucleic acids research* 2005; **33**(13)**:** 4140-4156.

20. Huesken D, Lange J, Mickanin C, Weiler J, Asselbergs F, Warner J *et al.* Design of a genome-wide siRNA library using an artificial neural network. *Nat Biotechnol* 2005; **23**(8)**:** 995-1001.

21. Sadler AJ, Williams BR. Interferon-inducible antiviral effectors. *Nature reviews* 2008; **8**(7)**:** 559-568.

22. Di Marco V, Craxi A. Chronic hepatitis B: who to treat and which choice of treatment? *Expert review of anti-infective therapy* 2009; **7**(3)**:** 281-291.

23. Webster DP, Klenerman P, Collier J, Jeffery KJ. Development of novel treatments for hepatitis C. *The Lancet infectious diseases* 2009; **9**(2)**:** 108-117.

24. Averett DR, Fletcher SP, Li W, Webber SE, Appleman JR. The pharmacology of endosomal TLR agonists in viral disease. *Biochemical Society transactions* 2007; **35**(Pt 6)**:** 1468-1472.

25. Arbuthnot P, Longshaw V, Naidoo T, Weinberg MS. Opportunities for treating chronic hepatitis B and C virus infection using RNA interference. *Journal of viral hepatitis* 2007; **14**(7)**:** 447-459.

26. Berkhout B, ter Brake O. Towards a durable RNAi gene therapy for HIV-AIDS. *Expert opinion on biological therapy* 2009; **9**(2)**:** 161-170.

27. Watanabe T, Umehara T, Kohara M. Therapeutic application of RNA interference for hepatitis C virus. *Advanced drug delivery reviews* 2007; **59**(12)**:** 1263-1276.

28. Robbins M, Judge A, Ambegia E, Choi C, Yaworski E, Palmer L *et al.* Misinterpreting the therapeutic effects of small interfering RNA caused by immune stimulation. *Human gene therapy* 2008; **19**(10)**:** 991-999.

29. Nguyen DN, Chen SC, Lu J, Goldberg M, Kim P, Sprague A *et al.* Drug Delivery-mediated Control of RNA Immunostimulation. *Mol Ther* 2009; advance online publication, July 7, 2009; doi:10.1038/mt.2009.147.

30. Morrissey DV, Lockridge JA, Shaw L, Blanchard K, Jensen K, Breen W *et al.* Potent and persistent in vivo anti-HBV activity of chemically modified siRNAs. *Nat Biotechnol* 2005; **23**(8)**:** 1002-1007.

31. Goodchild A, Nopper N, King A, Doan T, Tanudji M, Arndt GM *et al.* Sequence determinants of innate immune activation by short interfering RNAs. *BMC immunology* 2009; **10:** 40.

32. Matranga C, Tomari Y, Shin C, Bartel DP, Zamore PD. Passenger-strand cleavage facilitates assembly of siRNA into Ago2-containing RNAi enzyme complexes. *Cell* 2005; **123**(4)**:** 607-620.

33. Winter J, Jung S, Keller S, Gregory RI, Diederichs S. Many roads to maturity: microRNA biogenesis pathways and their regulation. *Nature cell biology* 2009; **11**(3)**:** 228-234.

34. Glasgow GM, McGee MM, Sheahan BJ, Atkins GJ. Death mechanisms in cultured cells infected by Semliki Forest virus. *The Journal of general virology* 1997; **78 (Pt 7):** 1559-1563.

35. Deuber SA, Pavlovic J. Virulence of a mouse-adapted Semliki Forest virus strain is associated with reduced susceptibility to interferon. *The Journal of general virology* 2007; **88**(Pt 7)**:** 1952-1959.

36. Ellery PJ, Tippett E, Chiu YL, Paukovics G, Cameron PU, Solomon A *et al.* The CD16+ monocyte subset is more permissive to infection and preferentially harbors HIV-1 in vivo. *J Immunol* 2007; **178**(10)**:** 6581-6589.

37. Zuker M. Mfold web server for nucleic acid folding and hybridization prediction. *Nucleic acids research* 2003; **31**(13)**:** 3406-3415.

Table 1 Sequences of ssRNAs used in the study

Name	Sequence	dG
B-406AS	5′UAAUUCGCGUCUGGCCUUCUU 3′	-0.5
B-406AS-1	5′UA**G**UU**G**GC**C**UCUGGCCUUCUU 3′	-5.6
B-406AS-2	5′UA**G**UU**G**GCGUCUGGCCUUCUU 3′	-4.0
B-406AS-3	5′UAAUU**G**GCGUCUGGCCUUCUU 3′	-3.9
ss41-N (Native)	5′GCCCGACAGAAGAGAGACAC 3′	-
ss41-L (Loop)	5′GCC**G**GACAGAAGAGAGAC**G**C 3′	1.3
ss41-2	5′GCC**G**GACA**UU**AGAGAGAC**G**C 3′	1.3
ss41-4	5′GCC**G**GACA**UU**A**U**A**U**AGAC**G**C 3′	1.3
ss41-6	5′GCC**G**GACA**UU**A**UUU**A**U**AC**G**C 3′	1.3
ss41-8	5′GCC**G**G**U**C**UUU**A**UUU**A**U**AC**G**C 3′	1.3
ss41-10	5′GCC**G**G**U**C**UUUUUUUUU**AC**G**C 3′	1.3

The modifications to the native sequences (either B-406AS or ss41-Native) are highlighted in bold.

Figure 1 Relative immunostimulation of ssRNAs with sequence or structural alterations.

(a) and (c) mFOLD-predicted structure of ssRNAs.[37] All ss41-RNAs have a similar predicted secondary structure and only ss41-loop and ss41-8 are presented here. The amount of uridines in the ss41 series is indicated by the x in the ss41-x name. Predicted free-energy of the loops is indicated with dG value. ss41-Native does not have a predicted secondary structure. All sequences are shown in Table 1. (**b) and (d)** Immunostimulation of ssRNAs in human PBMCs treated with 90 nM of indicated ssRNA complexed with DOTAP and incubated for 16 hours at 37°C. Cytokine production was measured by specific ELISA as described in *Materials and Methods*. The data is averaged from (**b)** three independent experiments in biological triplicate from four blood donors and **(d)** two independent experiments in biological triplicate from three blood donors. **(b)** Unpaired two-tailed T-test and non-parametric two-tailed Mann-Whitney test were used for IFN-α and TNF-α statistical comparison compared with B-406-AS, respectively. NS: non-significant.

Figure 2 Rational design of immunotimulatory siRNA scaffold.

(a) Overview of design approach. siLam-N is the original siRNA sequence targeting the *LaminA/C* mRNA. Watson-Crick base-pairing is shown with a "|" symbol, while G:U wobble pairing is indicated with a dot. The target-specific sequence of the guide strand is in italics, and the "GU" immunostimulatory motifs added to the native sequence are in bold. **(b)** Immunostimulation of siRNAs in human PBMCs treated with 600 nM of siRNA complexed with DOTAP and incubated for 16 hours at 37°C. Cytokine production was measured by specific ELISA. The data is averaged from three independent experiments in three different blood donors. Unpaired two-tailed non-parametric Mann-Whitney tests are versus siLam-N. **(c)** Knockdown

efficiency of siRNAs transfected in HEK 293 cells at a final concentration of 10 nM. After 24 hours at 37°C, total RNA was extracted and reverse-transcribed as described in *Material and Methods*. *LaminA/C* mRNA expression was assessed by quantitative real time PCR, and reported to that of *GAPDH*. The data is expressed as percentage of fold expression of siControl, and is averaged from two independent experiments in biological triplicate. Unpaired two-tailed T-test is presented using siLam-N as a reference.

Figure 3 Validation of uridine -bulge siRNA design scaffold.

(a) and (c) Human PBMCs were treated with indicated concentration of specified siRNA complexed with DOTAP and incubated for 16 hours at 37°C. Cytokine production was measured by specific ELISA. **(a)** The data is averaged from four independent experiments in four blood donors. Unpaired two-tailed non-parametric Mann-Whitney tests are shown. **(b)** RNAi efficiency of EGFP siRNAs. HEK 293 cells stably expressing EGFP were transfected with 10 nM of indicated siRNA for ~48 hours. EGFP production was assayed in fluorescent plate reader as described in *Materials and Methods*. The data is presented as the EGFP protein concentration relative to that of the Mock transfected control, and is averaged from three independent experiments in biological triplicate. siGFP19+2 is a 21 bp siRNA targeting EGFP.[4] Unpaired two-tailed T-test is presented using siEGFP-U as a reference. **(c)** The data is averaged from two blood donors in biological triplicate and is representative of two independent experiments. Unpaired two-tailed non-parametric Mann-Whitney tests are shown. **(d)** Knockdown efficiency of siRNAs transfected in Murine TC-1 cells at a final concentration of 10 nM. After 24 hours at 37°C, total RNA was extracted and reverse-transcribed as described in *Materials and Methods*. The *E6/E7* mRNA was assessed by quantitative real time PCR, and presented relative to that of mouse *GAPDH*. The data is expressed as percentage fold expression of siControl, and is averaged

from two independent experiments in biological triplicate. Unpaired two-tailed T-test comparing siE6/E7 and siE6/E7-U is shown using siE6/E7 as a reference. **(e)** Details of siEGFP and siE6/E7 designs. Watson-Crick base-pairing is shown with a "|" symbol, the 19 nt target-specific sequence of the guide strand is in italics, and the "U" bulge immunostimulatory motifs added to the native sequences are in bold.

Figure 4 Species-specific response to the uridine-bulge.

(a) FACS-purified CD14+ human monocytes and **(b)** mouse BMMs were stimulated with **(a)** 500 nM **(b)** or indicated concentration of specified siRNA complexed with DOTAP and incubated for 16 hours at 37°C. Cytokine production was measured by specific ELISA. **(a)** The data is averaged from two independent experiments in biological triplicate in two blood donors. Unpaired two-tailed non-parametric Mann-Whitney test comparing siEGFP and siEGFP-U is shown. **(b)** The data is representative of two independent experiments in biological triplicate.

Figure 5 Immunostimulatory profile of uridine-bulge modification.

(a)-(d) PBMCs from two blood donors were treated with 750 nM of indicated siRNA complexed with DOTAP in biological duplicate and incubated for 16 hours at 37°C. Cytokine concentrations were measured using 50 μl of supernatants with a 17 cytokines bead-array (BioRad) on a Bioplex platform. The data is averaged from two blood donors in biological duplicate, giving four data points per condition. Unpaired two-tailed T-tests were carried out for each siRNA pair, with or without the uridine modification.

Figure 6 Antiviral effects of the uridine-bulge-driven increased immunostimulation.

Human PBMCs were treated overnight with DOTAP-complexed siEGFP and its uridine-bulge variant (at 750 nM), and the supernatants collected. 100% confluent Hela cells were pre-treated with the resulting conditioned media for 4 hours, prior to infection with SFV, as described in *Materials and Methods*. Following 36 hours at 37°C, the cells were fixed, stained with crystal violet, and relative absorbance measured. Cell survival inversely correlates with viral activity, thereby resulting in increased absorbance readings when the antiviral effect is greater. The data is averaged from four independent viral assays, from two blood donors. Unpaired two-tailed T-test is presented comparing siEGFP and siEGFP-U conditions.

Figure 7 Conserved RNAi efficiency, but not increased immunostimulation, depends on the siRNA scaffold.

(a) Human PBMCs were treated with indicated concentration of specified siRNA complexed with DOTAP and incubated for 16 hours at 37°C. Cytokine production was measured by specific ELISA. The data is averaged from two blood donors in biological triplicate and is representative of two independent experiments. **(b)** HEK 293T cells were transfected with pLenti4/TO/V5-GW/*lacZ* for 16 hours at 37°C prior to transfection with 10 nM of indicated siRNA. 24 hours post-siRNA transfection, the cells were lysed and assayed for β-galactosidase activity as described in *Materials and Methods*. The data is averaged from two independent experiments in biological triplicate and expressed as percentage of the β-galactosidase activity of the Mock condition. Unpaired two-tailed T-test is presented compared to siβ-Gal-924.

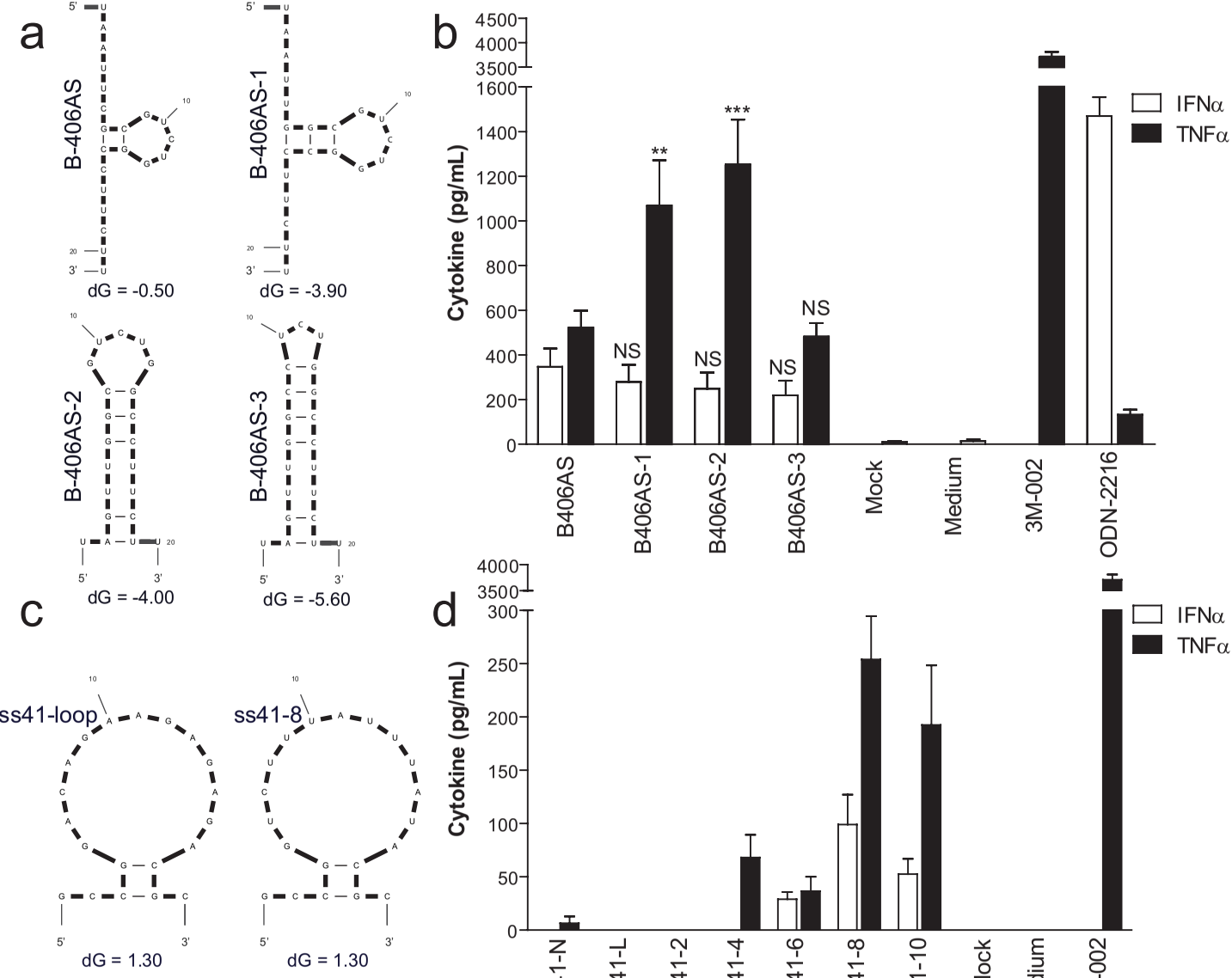
a
B-406AS
dG = -0.50
B-406AS-1
dG = -3.90
B-406AS-2
dG = -4.00
B-406AS-3
dG = -5.60
b
Cytokine (pg/mL)
IFNα
TNFα
**
***
NS
B406AS
B406AS-1
B406AS-2
B406AS-3
Mock
Medium
3M-002
ODN-2216
c
ss41-loop
dG = 1.30
ss41-8
dG = 1.30
d
Cytokine (pg/mL)
IFNα
TNFα
ss41-N
ss41-L
ss41-2
ss41-4
ss41-6
ss41-8
ss41-10
Mock
Medium
3M-002

Figure 1

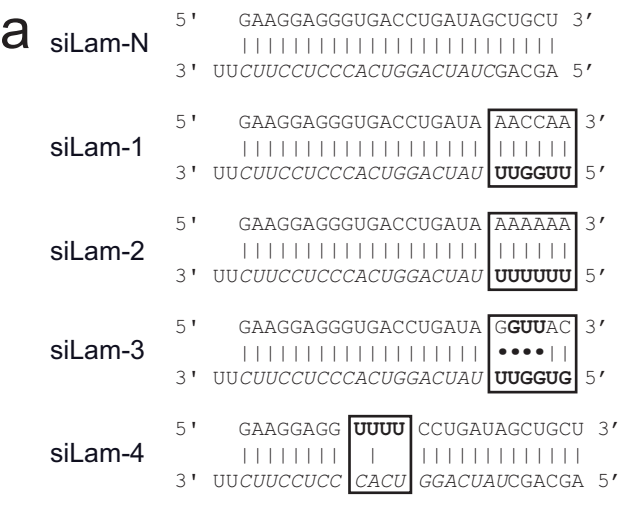
a
siLam-N
5' GAAGGAGGGUGACCUGAUAGCUGCU 3'
3' UUCUUCCUCCCACUGGACUAUCGACGA 5'
siLam-1
5' GAAGGAGGGUGACCUGAUA AACCAA 3'
3' UUCUUCCUCCCACUGGACUAU UUGGUU 5'
siLam-2
5' GAAGGAGGGUGACCUGAUA AAAAAA 3'
3' UUCUUCCUCCCACUGGACUAU UUUUUU 5'
siLam-3
5' GAAGGAGGGUGACCUGAUA GGUUAC 3'
3' UUCUUCCUCCCACUGGACUAU UUGGUG 5'
siLam-4
5' GAAGGAGG UUUU CCUGAUAGCUGCU 3'
3' UUCUUCCUCC CACU GGACUAUCGACGA 5'

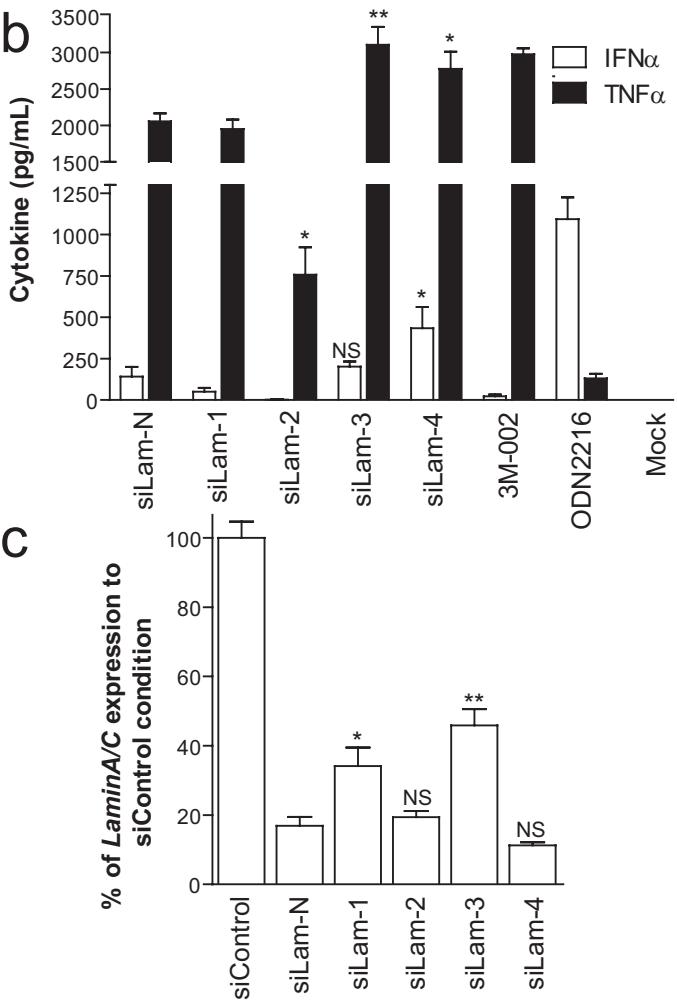
b
Cytokine (pg/mL)
IFNα
TNFα
NS
siLam-N
siLam-1
siLam-2
siLam-3
siLam-4
3M-002
ODN2216
Mock
c
% of LaminA/C expression to siControl condition
siControl
siLam-N
siLam-1
siLam-2
siLam-3
siLam-4

Figure 2

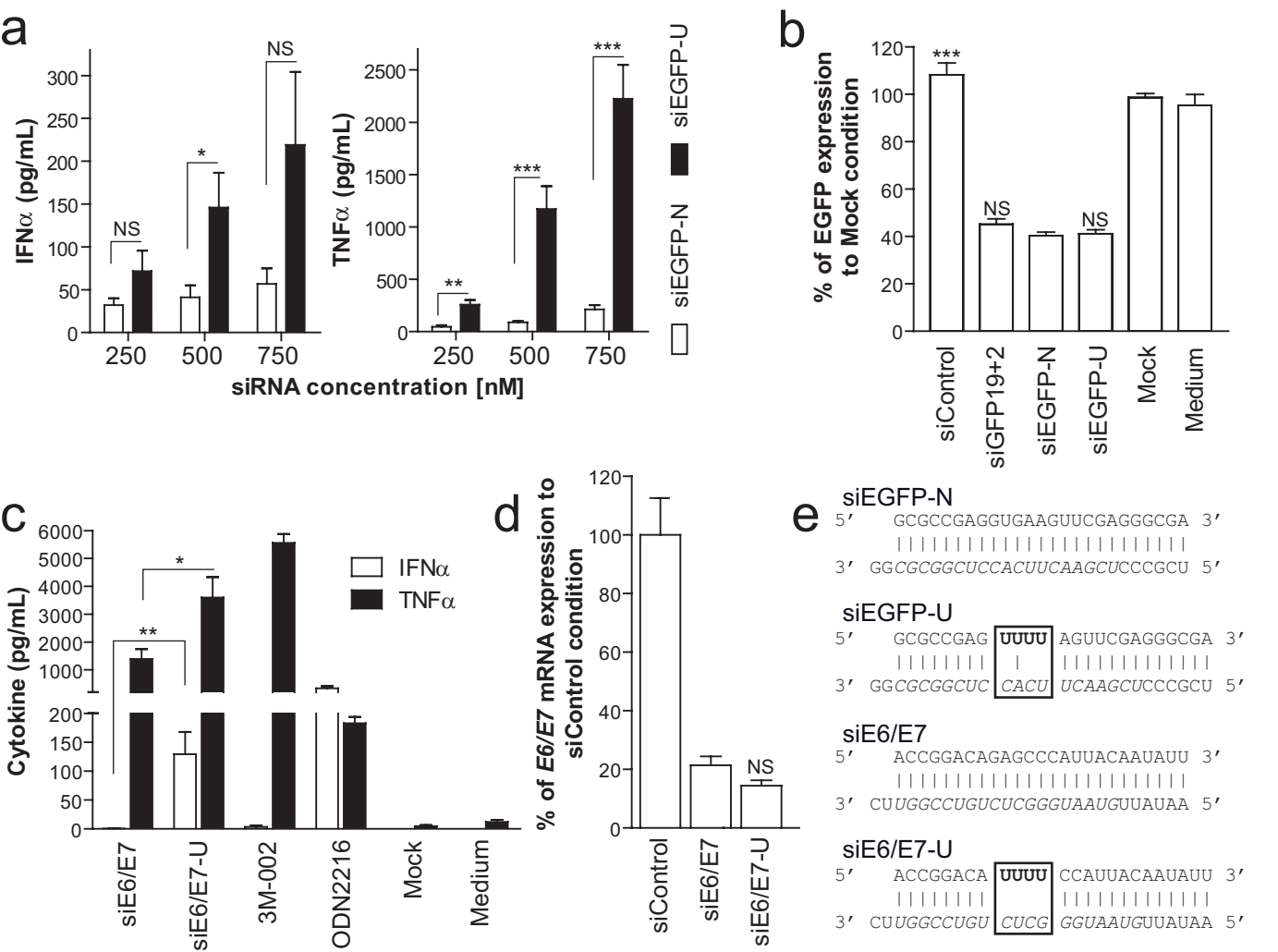
a
IFNα (pg/mL)
TNFα (pg/mL)
NS
*
**
***
siEGFP-U
siEGFP-N
250
500
750
siRNA concentration [nM]
b
% of EGFP expression to Mock condition
siControl
siGFP19+2
siEGFP-N
siEGFP-U
Mock
Medium
c
Cytokine (pg/mL)
IFNα
TNFα
siE6/E7
siE6/E7-U
3M-002
ODN2216
Mock
Medium
d
% of E6/E7 mRNA expression to siControl condition
siControl
siE6/E7
siE6/E7-U
e
siEGFP-N
5′ GCGCCGAGGUGAAGUUCGAGGGCGA 3′
3′ GGCGCGGCUCCACUUCAAGCUCCCGCU 5′
siEGFP-U
5′ GCGCCGAG UUUU AGUUCGAGGGCGA 3′
3′ GGCGCGGCUC CACU UCAAGCUCCCGCU 5′
siE6/E7
5′ ACCGGACAGAGCCCAUUACAAUAUU 3′
3′ CUUGGCCUGUCUCGGGUAAUGUUAUAA 5′
siE6/E7-U
5′ ACCGGACA UUUU CCAUUACAAUAUU 3′
3′ CUUGGCCUGU CUCG GGUAAUGUUAUAA 5′

Figure 3

Figure 4

a
TNFα (pg/mL)
0
100
200
300
400
500
siEGFP-N
siEGFP-U
Mock
Medium
**
b
mTNFα (pg/mL)
0
500
1000
1500
2000
2500
10000
11000
siEGFP-N
siEGFP-U
Mock
3M-002
750 nM
500 nM
250 nM

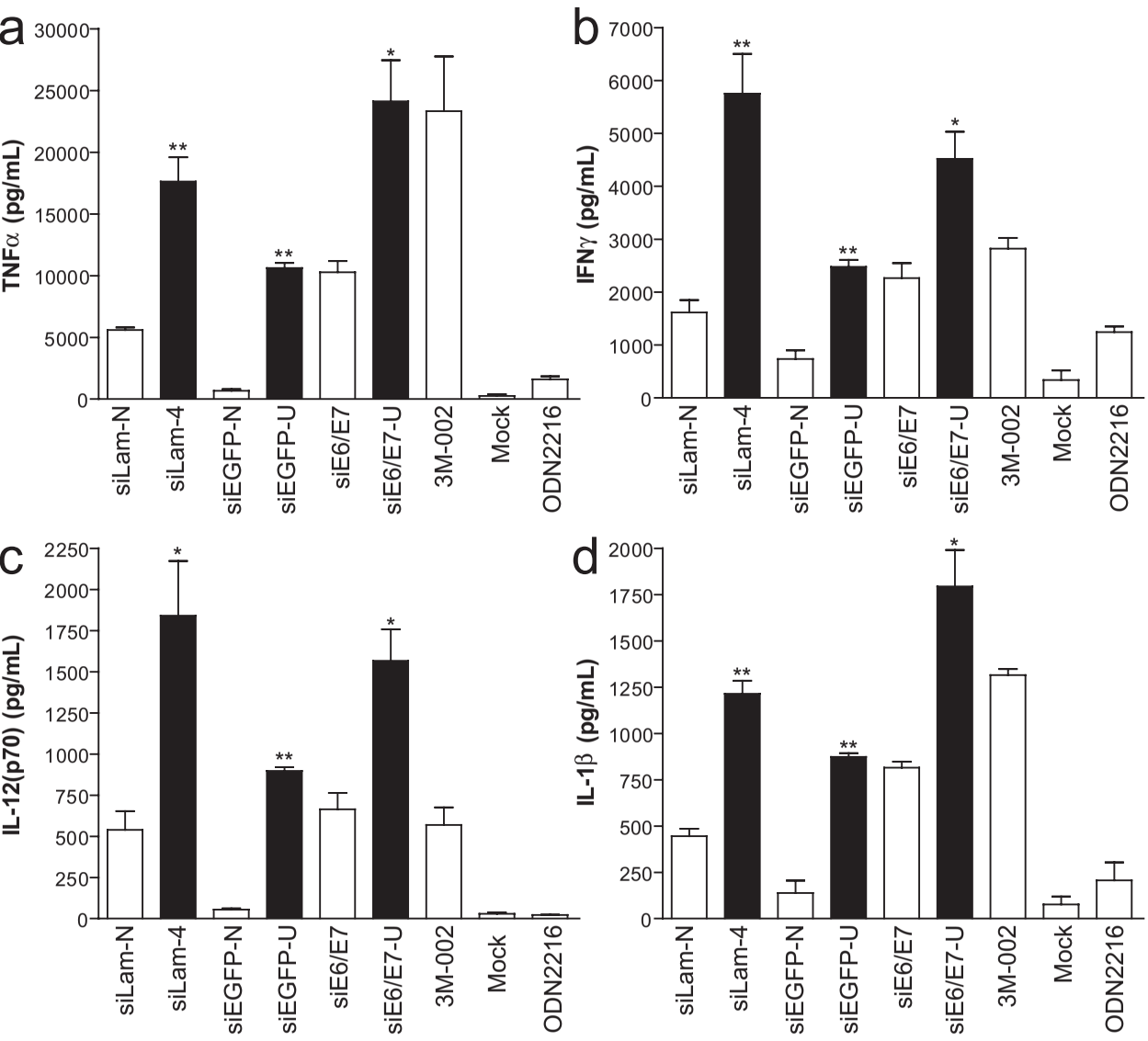
a
TNFα (pg/mL)
30000
25000
20000
15000
10000
5000
0
b
IFNγ (pg/mL)
7000
6000
5000
4000
3000
2000
1000
0
c
IL-12(p70) (pg/mL)
2250
2000
1750
1500
1250
1000
750
500
250
0
d
IL-1β (pg/mL)
2000
1750
1500
1250
1000
750
500
250
0
siLam-N
siLam-4
siEGFP-N
siEGFP-U
siE6/E7
siE6/E7-U
3M-002
Mock
ODN2216

Figure 5

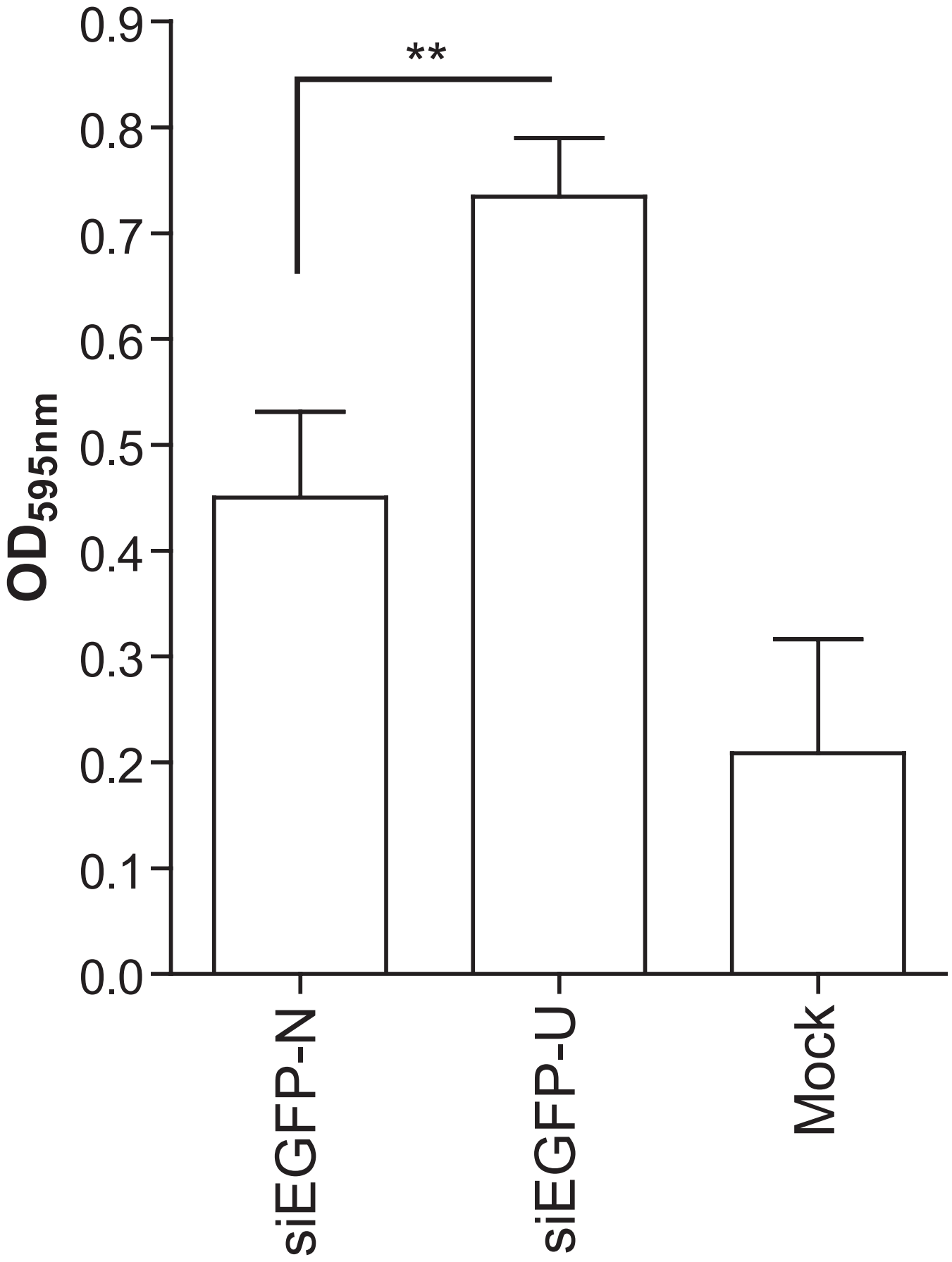

Figure 6

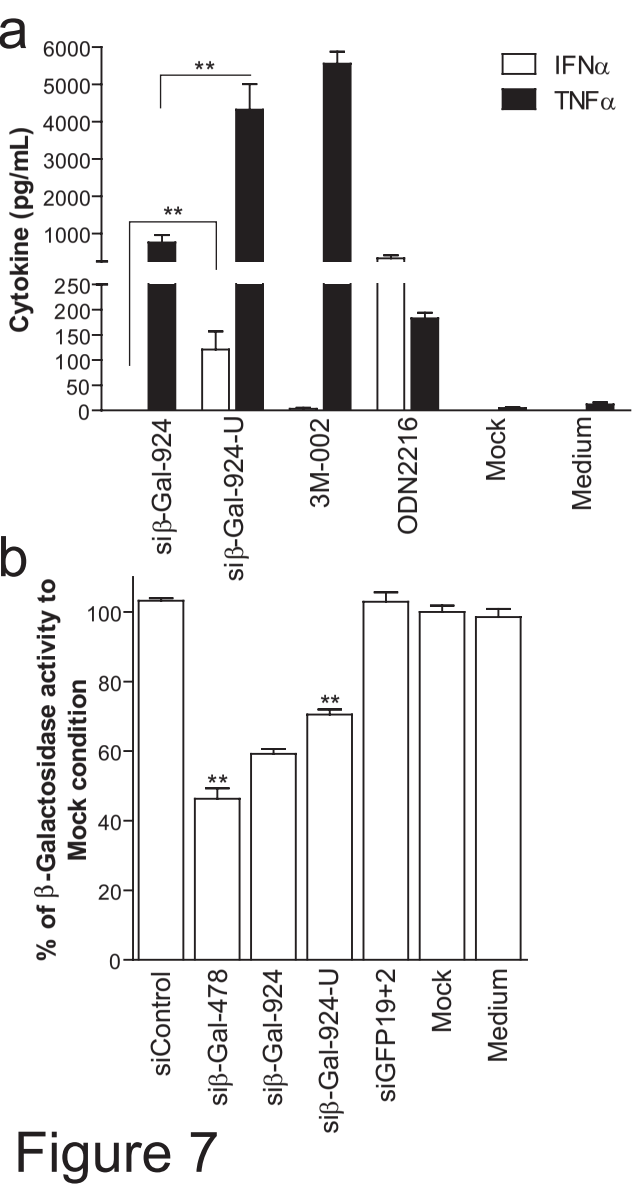
a
Cytokine (pg/mL)
6000
5000
4000
3000
2000
1000
250
200
150
100
50
0
**
**
IFNα
TNFα
siβ-Gal-924
siβ-Gal-924-U
3M-002
ODN2216
Mock
Medium
b
% of β-Galactosidase activity to Mock condition
100
80
60
40
20
0
**
**
siControl
siβ-Gal-478
siβ-Gal-924
siβ-Gal-924-U
siGFP19+2
Mock
Medium

Figure 7

Figure S1

TNFα (pg/mL)
0
2000
4000
6000
8000
siEGFP-N
siEGFP-U
siBcl2l12-N
siBcl2l12-U
3M-002
Mock
750 nM
500 nM
250 nM